Optimized prefactored compact schemes for wave propagation phenomena

I. Spisso*, A. Rona**, E. Hall**, M. Bernardini***, S. Pirozzoli***

*i.spisso@cineca.it, HPC consultant for academic and industrial CFD applications
SuperComputing Applications and Innovation Department,CINECA, via Magnanelli 6/3, 40033 Casalecchio di Reno, Italy
**Department of Engineering, University of Leicester, Leicester, LE1 7RH, England
***Department of Mechanical & Aerospace Engineering, Università degli Studi di Roma La Sapienza, Via Eudossiana 18, 00184 Roma, Italy

13 September 2016, Milano, Italy

SIMAI Conference

Outline of the presentation

1. Context, Aim and Objectives
   - Context
   - Aim and Objectives
2. Numerical Background
   - Model problem
   - Spatial Discretization
   - Time marching scheme
   - Performance analysis of finite-difference schemes
   - Cost-performance trade-off for CAA algorithms
   - Approximate spatial and temporal error analysis
3. Optimization criteria
   - Optimization of finite-difference schemes
   - Extension to prefactored schemes
   - Optimization of the temporal solver
   - Predicted performance of the combined schemes
4. Applications
   - Polychromatic wave propagation
   - One-dimensional Gaussian pulse
   - 1D performance analysis summary
   - Two-dimensional Gaussian pulse
   - 2D performance analysis summary
5. Conclusion
6. Track record on cost-optimized schemes and further/on-going work

Context I

What is Computational AeroAcoustics (CAA)

CAA concerns with the accurate numerical prediction of aerodynamically generated noise as well as its propagation and far-field characteristics.

Example: scattering problems (trailing/leading edge noise, modal scattering in turbomachinery blade row), non-linear problems of flow acoustics (high-speed jet noise)

Context II

Challenges in modelling wave generation and propagation phenomena

- Aeroacoustic problems are inherently unsteady by definition
- Aeroacoustic problems typically involve frequencies over a wide bandwidth.
- Acoustic waves usually have small amplitudes. They are very small compared to the mean flow dynamic pressure. Often, the sound intensity is five to six orders smaller than dynamic pressure.
- In most aeroacoustic problems, interest is in the sound waves radiated to the far field. This requires a solution that is uniformly valid from the source region all the way to the measurement point many acoustic wavelengths away.
- CAA algorithms must have minimal numerical dispersion and dissipation.
- Stable and accurate boundary conditions are of utmost importance in CAA.

Aim and Objectives I

Aim of the present work

- To develop a novel algorithm based on the prefactoriztion of [?] to reduce the computational cost for a given level of error [?].
- To evaluate the line solver kernel performance for the propagation of one- and two-dimensional perturbations.

Objectives

- Formulate and implement an optimization procedure for the spatial differentiation and the temporal integration of time-marching pre-factored compact centred finite-difference schemes;
- Test the procedure on the bi-diagonal prefactored compact scheme of [?] and evaluate its performance with respect to the same scheme optimized for maximum formal accuracy;
- Test the variation in scheme performance with the number of spatial dimensions.

Outline of the presentation

1. Context, Aim and Objectives
   - Context
   - Aim and Objectives
2. Numerical Background
   - Model problem
   - Spatial Discretization
   - Time marching scheme
   - Performance analysis of finite-difference schemes
   - Cost-performance trade-off for CAA algorithms
   - Approximate spatial and temporal error analysis
3. Optimization criteria
   - Optimization of finite-difference schemes
   - Extension to prefactored schemes
   - Optimization of the temporal solver
   - Predicted performance of the combined schemes
4. Applications
   - Polychromatic wave propagation
   - One-dimensional Gaussian pulse
   - 1D performance analysis summary
   - Two-dimensional Gaussian pulse
   - 2D performance analysis summary
5. Conclusion
6. Track record on cost-optimized schemes and further/on-going work

Model problem I

Model problem: Linear Advection Equation (LAE) of sinusoidal disturbance

$$\frac{\partial f}{\partial t} + c\frac{\partial f}{\partial x} = 0, \qquad f(x,0) = \hat{f}_0 e^{\mathbf{i}kx}, \tag{1}$$

- with wavelength λ, wavenumber $k = 2\pi/\lambda$, and scaled wavenumber $\kappa = kh$
- uniformly discretized both in space (grid spacing h) and time (time step Δt)
- method of lines, two-stages discretization

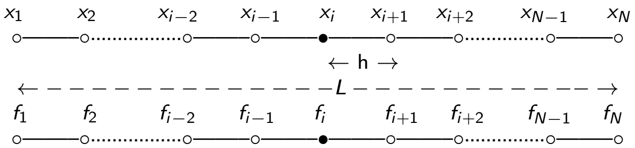

Figure: 1. Variation of discrete function $f_i = f(x_i)$ along uniformly discretised length L.

Spatial Discretization I

Finite-difference spatial discretization

The finite difference approximation f_i' to the first derivative $\dfrac{\partial f(x_i)}{\partial x}$ at node i, using a $(R+S+1)$ point stencil, depends on the function values at the nodes near i of [?]:

$$\sum_{j=-P}^{Q} \alpha_j \, f'_{i+j} = \frac{1}{h} \sum_{j=-R}^{S} a_j \, f_{i+j} + O(h^n), \tag{2}$$

The spatial scheme is $CPQRS$. If $P = Q = 0$, then the scheme is explicit. Implicit or compact schemes have $(P \vee Q) \neq 0$

Taking the Fourier transform of both sides of eq. (2) gives:

$$\bar{\kappa}\,(\kappa) = \bar{k}\,(k)\,h = \frac{1}{\mathrm{i}} \frac{\sum_{j=-R}^{S} a_j e^{\mathrm{i}\,j\,\kappa}}{\sum_{j=-P}^{Q} \alpha_j e^{\mathrm{i}\,j\,\kappa}}, \tag{3}$$

where $\bar{\kappa} = \bar{k}\,h$ is the scaled pseudo-wavenumber. The scaled wavenumber κ and the scaled pseudo-wavenumber $\bar{\kappa}$ are both non-dimensional values, $\kappa \in \mathbb{R}$, $0 < |\kappa| \leq \pi$, and generally $\bar{\kappa} \in \mathbb{C}$, with real and imaginary part $\Re[\bar{\kappa}]$ and $\Im[\bar{\kappa}]$.

Scaled pseudo-wavenumber diagram

- It is desirable to make $\bar{\kappa}$ equal to κ. It is impossible to build up a perfect match between $\bar{\kappa}$ and κ over the entire wavenumber range due to the limitation of numerical discretization.
- In practice, the scaled pseudo-wavenumber $\bar{\kappa}$ implies a certain deviation from the true scaled wavenumber κ, which increases as $\kappa \to \pi$ (for $\kappa = \pi$, $\bar{\kappa} = 0$)
- This deviation results in spatial numerical error $e_0(\kappa)$, where the real part represent the dispersive error $\varepsilon_R(\kappa)$ and the imaginary part the dissipative error $\varepsilon_I(\kappa)$
- the coefficients α_j, a_j that appear in eq. (2) are chosen to give the largest possible order of accuracy or to reduce the dispersive and dissipative error [**?**]

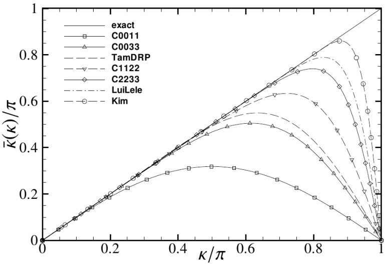

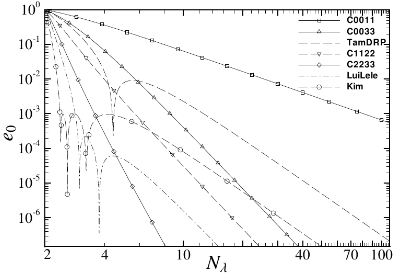

Time marching scheme I

Runge-Kutta schemes

Runge-Kutta schemes are considered as time-advancing schemes in the present work [**?**].
An explicit p-stage, single-step, two-level, RK scheme advances the solution from the time level $t = t_n$ to $t_n + \Delta t$ as

$$\mathbf{U}^{n+1} = \mathbf{U}^n + \sum_{j=1}^{p} \gamma_j \, \Delta t^j \, \frac{\partial^j \mathbf{U}^n}{\partial t^j}, \tag{4}$$

- $\mathbf{U}$ represents the vector containing the solution values at spatial mesh nodes
- γ_j are the coefficients of the RK algorithm with

$$\gamma_j = \prod_{l=p-j+1}^{p} \alpha_l \qquad \text{for} \quad j = 1, \ldots, p. \tag{5}$$

- the coefficients γ_j that appear in eq. (5) are chosen to give the maximum order of accuracy ($\gamma_m = \frac{1}{m!} \;\; m = 1, \cdots, p$) for a given p-stage RK scheme, or to minimize the temporal dissipation and phase error [**?**]

Time marching scheme II

Amplification factor and stability limit of the algorithm

Applying a temporal Fourier transform to eq. (4), the amplification factor of the algorithm is obtained as [**?**]:

$$r\left(\kappa,\sigma\right) = 1 + \sum_{j=1}^{p} \gamma_j \left(-\mathrm{i}\,\sigma\,\bar{\kappa}\left(\kappa\right)\right)^j, \tag{6}$$

where σ is the Courant number:

$$\sigma = \frac{c\Delta t}{h}. \tag{7}$$

The amplification factor in the case of null spatial error, for which $\bar{\kappa} = \kappa$ in eq. (3), is:

$$r_t\left(z,\gamma_j\right) = 1 + \sum_{j=1}^{p} \gamma_j \left(-\mathrm{i}\,z\right)^j \tag{8}$$

with $z = \sigma\kappa \in \mathbb{C}$ complex plane. The stability limit z_s is given by the following condition:

$$z_s = \max\left\{z,\ |r_t(z,\gamma_j)| \leq 1\right\}. \tag{9}$$

The linear FD approximation of eq. (1) has the approximate solution

$$v(x,T) = \hat{u}_0\, e^{\mathrm{i}kx} r^n. \tag{10}$$

Performance analysis of finite-difference schemes

Normalized error and computational cost metrics

Following [?], let E be the relative L_2 error norm at time $T = n\Delta t$:

$$E = \frac{|v(\cdot\,,T) - u(\cdot\,,T)|_2}{|u_0(\cdot\,)|_2} = (ckT)\cdot\frac{|r\,(\kappa,\sigma) - e^{-\mathbf{i}\sigma\kappa}|}{\sigma\kappa}, \tag{11}$$

where $n = (ckT)\,/\,(\sigma\kappa)$
The computational cost C of solving numerically eq. (10) is assumed to be proportional to: the total number of points, L/h, the number of operations per node N_{op} required by the spatial discretization, the number of RK stages p, the number of time steps $n = T/\Delta t$ [?]. This gives:

$$C \propto pN_{op}TL\frac{1}{\Delta t\,h} = pN_{op}\cdot(ckT)\cdot(kL)\cdot\frac{1}{\sigma\kappa^2}. \tag{12}$$

It is possible to derive, with a few approximations, the expression for the normalized cost and error metrics:

$$e(\kappa,\sigma) \equiv \frac{E}{(ckT)} = \frac{|r\,(\kappa,\sigma) - e^{-\mathbf{i}\sigma\kappa}|}{\sigma\kappa}, \tag{13a}$$

$$c_1(\kappa,\sigma) \equiv \frac{C}{(ckT)\cdot(kL)} = pN_{op}\,\frac{1}{\sigma\kappa^2}. \tag{13b}$$

Cost-performance trade-off for CAA algorithms I

Cost-optimal condition for single scale problems

Optimizing the performance of a given scheme (i.e. for given values of p, N_{op}), for a given problem (i.e. for a given value of ckT, kL) requires that the computational cost is minimum for a given error level.
This can be done by specifying a target level for the relative error, say ϵ, which implies

$$e(\kappa,\sigma) = \frac{\epsilon}{ckT} \equiv \tilde{\epsilon}, \tag{14}$$

and finding a pair of values $(\kappa^*(\tilde{\epsilon}), \sigma^*(\tilde{\epsilon}))$ that minimize the cost metric and that satisfy both the stability limitation $|r(\kappa,\sigma)| \leq 1,\ \forall \kappa \in [0,\pi]$ and the limitation on the maximum value of Courant number $\sigma \leq \sigma_{max}$:

$$\sigma_{max} = \frac{z_s}{\max\limits_{\kappa\in(0,\pi)} \bar{\kappa}\,(\kappa)}, \tag{15}$$

A graphical interpretation of the the optimization problem is given by inspection of the iso-lines $e(\kappa,\sigma)$ and $c(\kappa,\sigma)$ in the (κ,σ) plane, as shown in the next slide for $C1122/RK4$ scheme.

Cost-performance trade-off for CAA algorithms II

Iso-error and Iso-cost curves

- For any specified value of $\tilde{\epsilon}$, a pair of values (κ^*, σ^*) is sought to minimize $\dfrac{1}{\sigma\kappa^2}$ and which corresponds to the tangency point of the two families of curves
- Iso-error $\rightarrow$ solid line. Iso-cost $\rightarrow$ dashed lines
- The normalized cost function is concave and the normalized error function is (almost always) convex in the $[\kappa, \sigma]$ plane, therefore for any iso-error curve there is a unique point in which a curve of the iso-cost family is tangent to it [**?**].

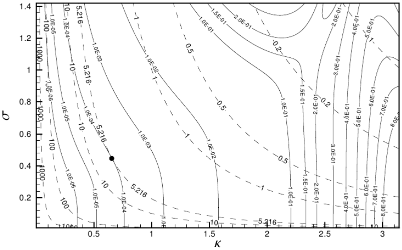

Optimal performance for multi-scale problems

- Aeroacoustic signals are typically broadband and can feature a range of propagating velocities c.
- Provided the spectrum can be taken as of finite width $|k| < \hat{k}$ and $|c| < \hat{c}$, the normalized cost and error metrics for a bandwidth-limited signal is estimated as:

$$c_d(\hat{\kappa}, \hat{\sigma}) \equiv p N_{op} \frac{1}{\hat{\sigma} \hat{\kappa}^{d+1}}, \tag{16a}$$

$$\hat{e}_a(\hat{\kappa}, \hat{\sigma}) \equiv \max(\hat{e}_0(\hat{\kappa}), \hat{e}_t(\hat{z})). \tag{16b}$$

where d is the number of spatial dimensions, N_{op} the number of operations per mesh node, $\hat{\kappa} = \hat{h}h$, $\hat{\sigma} = \hat{c}\Delta t/h$, $\hat{z} = \hat{\sigma}\hat{\kappa}$. $\hat{e}_0(\hat{\kappa})$ and $\hat{e}_t(\hat{z})$ are

$$\hat{e}_0(\hat{\kappa}) \equiv \frac{1}{\hat{\kappa}} \max_{0 \le \kappa \le \hat{\kappa}} |\bar{\kappa} - \kappa|, \tag{17a}$$

$$\hat{e}_t(\hat{z}) \equiv \frac{1}{\hat{z}} \max_{0 \le z \le \hat{z}} \left| \sum_{j=0}^{p} (-\mathrm{i}z)^j - \mathrm{e}^{-\mathrm{i}z} \right|. \tag{17b}$$

Approximate spatial and temporal error analysis I

Approximate spatial and temporal error analysis

- [?] has shown that, with a good approximation

$$e(\kappa,\sigma) \approx \max(e_0(\kappa), e_t(z)). \tag{18}$$

- where $e_0(\kappa)$ is the spatial error, the error in case of exact time integration, defined in eq. (19) [?]. $e_0(\kappa)$ is shown by the vertical long-dash dark line,
- and $e_t(z)$ is the temporal error, the error in case of exact space integration, defined in eq. (20) [?]. $e_t(z)$ is shown by the light blue line.

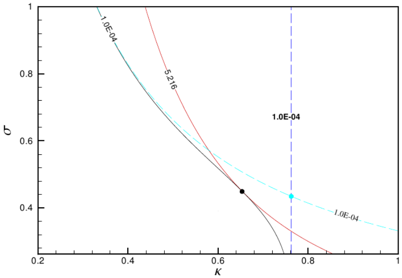

$$\underset{\sigma\to 0}{e(\kappa,\sigma)} \equiv e_0(\kappa), \tag{19}$$

$$\underset{\bar{\kappa}=\kappa}{e(\kappa,\sigma)} \equiv e_t(z) = \frac{\left| r_t\left(z,\gamma_j\right) - e^{-\mathbf{i}z} \right|}{z}, \tag{20}$$

Approximate spatial and temporal error analysis II

Spatial and Temporal resolving efficiency

The problem of determining the optimal performance of a given scheme can be approximately decoupled into two sub-problems, by considering the influence of space and time discretization separately, by

- computing the optimal reduced wavenumber according to

$$\check{\kappa}^*(\tilde{\epsilon}) \equiv \check{e}_0^{-1}(\tilde{\epsilon}) \tag{21}$$

- and computing the optimal Courant number by:

$$\check{\sigma}^*(\tilde{\epsilon}) = \check{z}^*(\tilde{\epsilon})/\check{\kappa}^*(\tilde{\epsilon}); \quad \check{z}^*(\tilde{\epsilon}) \equiv \check{e}_t^{-1}(\tilde{\epsilon}); \tag{22}$$

The quantities $\check{\kappa}^*(\tilde{\epsilon})$ and $\check{z}^*(\tilde{\epsilon})$ will be denoted, respectively, as 'spatial resolving efficiency' and 'temporal resolving efficiency' for a given value of normalized error $\tilde{\epsilon}$. The associated 'optimal' normalized cost is

$$\tilde{c}(\tilde{\epsilon}) = c_{n_D}(\check{\kappa}^*(\tilde{\epsilon}), \check{z}^*(\tilde{\epsilon})) = pN_{op}\,\frac{1}{\check{\sigma}^*\check{\kappa}^{*\,n_D+1}}. \tag{23}$$

Equations (18) allows to consider the spatial and temporal discretization separately in the present analysis to develop cost-optimized schemes.

Outline of the presentation

1. Context, Aim and Objectives
    - Context
    - Aim and Objectives
2. Numerical Background
    - Model problem
    - Spatial Discretization
    - Time marching scheme
    - Performance analysis of finite-difference schemes
    - Cost-performance trade-off for CAA algorithms
    - Approximate spatial and temporal error analysis
3. Optimization criteria
    - Optimization of finite-difference schemes
    - Extension to prefactored schemes
    - Optimization of the temporal solver
    - Predicted performance of the combined schemes
4. Applications
    - Polychromatic wave propagation
    - One-dimensional Gaussian pulse
    - 1D performance analysis summary
    - Two-dimensional Gaussian pulse
    - 2D performance analysis summary
5. Conclusion
6. Track record on cost-optimized schemes and further/on-going work

Optimization of finite-difference schemes I

Tridiagonal compact scheme C1122

- The optimization is achieved by maximizing the 'spatial resolving efficiency' $\check{\kappa}^*(\tilde{\epsilon})$.
- The authors have adopted as baseline spatial scheme the $C1122$ where α_1 is a free-parameter. With $\alpha_1 = 1/3$ the sixth-order $C1122$ scheme is obtained.

$$\alpha_1 f'_{i-1} + f'_i + \alpha_1 f'_{i+1} = \frac{1}{h}\left(a_{-2}f_{i-2} + a_{-1}f_{i-1} + a_1 f_{i+1} + a_2 f_{i+2}\right) + O(h^4), \qquad (24)$$

- The new class of schemes is labelled as $C1122$epsm$n$, where n is $\tilde{\epsilon} = 10^{-n}$.
- The optimal value of α_1 is plotted with solid line. The non-optimal $\check{\kappa}^*$ by the dashed-line, and the optimal $\check{\kappa}^*$ by the dashed-dotted line.
- Cost-optimized spatial discretizations can outperform a $C1122$ sixth-order scheme, yielding a 40% to 50% increase in $\check{\kappa}^*(\tilde{\epsilon})$.

$$\begin{cases} a_2 = -a_{-2} = \dfrac{1}{12}(4\alpha_1 - 1) \\ a_1 = -a_{-1} = \dfrac{1}{3}(\alpha_1 + 2) \end{cases} \qquad (25)$$

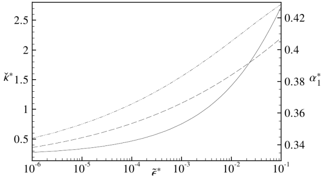

Optimization of finite-difference schemes II

Maximising the spatial resolving efficiency

- $\mathrm{C1122}$ is the baseline scheme, with the free parameter α_1.
- For a target level of error $\tilde{\epsilon} = \hat{e}_a = 10^{-n}$, find α_1 that maximises $\hat{\kappa}$.
- $(\alpha_1^n, \hat{\kappa}^n_{opt})$ are determined for the range $10^{-6} \le \hat{e}_a \le 10^{-4}$.

Table: 1. Coefficients and resolving efficiencies of optimised spatial C1122–n schemes.

	C1122–n		C1122	
n	α_1^n	$\hat{\kappa}^n_{\rm opt}$	α_1	$\hat{\kappa}^n$
4	0.354740	1.121	1/3	0.762
5	0.337838	0.776	1/3	0.522
6	0.335419	0.533	1/3	0.357

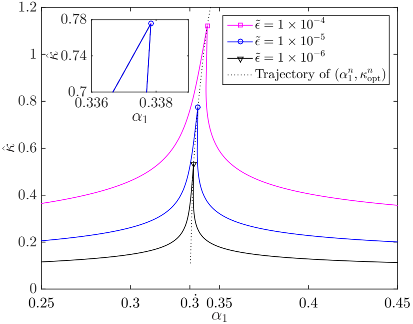

Figure: 2. Iso-lines of $\hat{e}_0$ $(\hat{\kappa})$ with varying α_1. Symbols show optimised α_1. Dotted line shows the α_1^n locus that asymptotes to $\alpha_1 = 1/3$.

Extension to prefactored schemes

Prefactored compact finite difference schemes

- To obtain the finite difference approximation $f_i^{'}$ from equation (24), a tridiagonal linear system of the form $Ax = b$ has to be solved.
- An alternative approach to the inversion of the A matrix has been proposed by [**?**], consisting in a prefactorization that splits the derivative operator $f_i^{'}$ in a backward component $f_i^{\prime B}$ and a forward component $f_i^{\prime F}$.
- This way, the inversion of the matrix is replaced by two independent matrix operations that involve bi-diagonal matrices.
- This class of prefactored schemes has been optimized by [**?**].
- To derive the cost-optimized prefactored compact schemes, the authors follow from previous work of [**?**] using the properties of the the MacCormack scheme.

Optimization of the temporal solver

Maximising the temporal resolving efficiency

- RK4 is the baseline time integration scheme, with γ_3 and γ_4 as free parameters.
- For the same target error $\tilde{\epsilon} = \hat{e}_a = 10^{-n}$, find γ_3 and γ_4 that maximise $\hat{z}$.
- $\left(\gamma_3^n, \gamma_4^n, \hat{z}_{opt}^n\right)$ are determined for the range $10^{-6} \leq \hat{e}_a \leq 10^{-4}$.

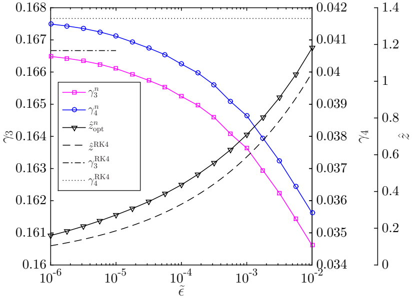

Figure: 3. Optimized RK4 and corresponding temporal resolving efficiency $\hat{z}_{opt}^n$ for a range of target errors $\tilde{\epsilon} = 10^{-n}$.

Table: 2. Coefficients and resolving efficiencies of optimised temporal RK4–n schemes.

	RK4–n				RK4			
n	γ_3^n	γ_4^n	z_s^n	$\hat{z}_{\mathrm{opt}}^n$	γ_3	γ_4	z_s	$\hat{z}^n$
4	0.165242	0.0402486	2.826	0.436	1/6	1/24	2.83	0.331
5	0.166106	0.0411119	2.828	0.272	1/6	1/24	2.83	0.186
6	0.166486	0.0414859	2.829	0.160	1/6	1/24	2.83	0.105

Dispersive spatial error characteristics I

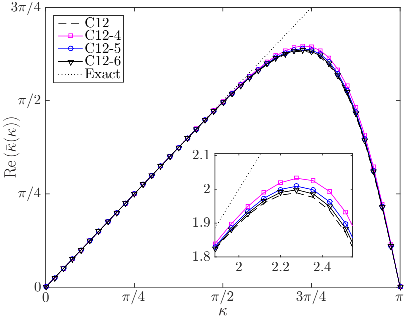

Figure: 4. Real component of non-dimensional wavenumber $\bar{\kappa}$ from the prefactored compact schemes.

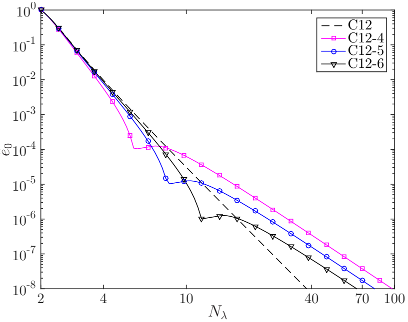

Figure: 5. Spatial error $\hat{e}_0$ versus number of points per wavelength N_λ.

Combined spatial and temporal error characteristics

- Combined space and time cost-optimization schemes for the same level of error $\tilde{\epsilon}$ have been developed, labelled as epsm$n$, where n is $\tilde{\epsilon} = 10^{-n}$.
- A computational advantage is predicted by using cost-optimized schemes to model wave propagation problems at their design operational points.
- The suggestion is to use the cost-optimized schemes at their design level of error and not beyond the intercept with their classical counterpart scheme.

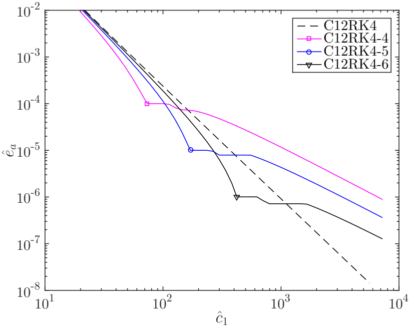

Figure: 6. Estimated error $\hat{e}_a$ versus computational cost $\hat{c}_1$ for the C12RK4-n schemes, one-dimensional implementation.

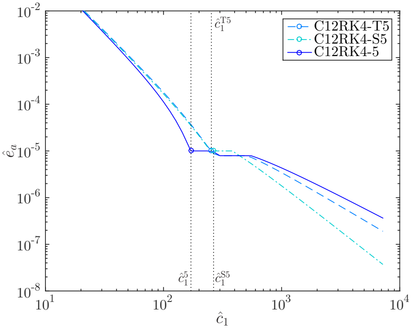

Figure: 7. Comparison of the estimated error $\hat{e}_a$ versus computational cost $\hat{c}_1$ among C12RK4-5, C12RK4-S5, and C12RK4-T5 schemes.

Outline of the presentation

1. Context, Aim and Objectives
   - Context
   - Aim and Objectives
2. Numerical Background
   - Model problem
   - Spatial Discretization
   - Time marching scheme
   - Performance analysis of finite-difference schemes
   - Cost-performance trade-off for CAA algorithms
   - Approximate spatial and temporal error analysis
3. Optimization criteria
   - Optimization of finite-difference schemes
   - Extension to prefactored schemes
   - Optimization of the temporal solver
   - Predicted performance of the combined schemes
4. Applications
   - Polychromatic wave propagation
   - One-dimensional Gaussian pulse
   - 1D performance analysis summary
   - Two-dimensional Gaussian pulse
   - 2D performance analysis summary
5. Conclusion
6. Track record on cost-optimized schemes and further/on-going work

Polychromatic wave propagation

Analytical formulation

- Numerical solution of the linear advection equation

$$\frac{\partial u}{\partial t} + c\frac{\partial u}{\partial x} = 0, \quad u(x,0) = u_0(x), \tag{26}$$

- Periodic boundary conditions $u(0,t) = u(1,t),\ t > 0$.
- Initial condition $u(x,0) = \sum_{j=1}^{4} \sin(2^{(j+1)}\pi x)$.
- Error $\bar{e}$ computed as the normalised relative $L2$ norm of $u_h(x_i,T) - u(x_i,T)$.

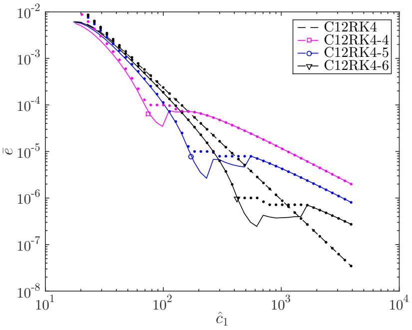

Figure: 8. Computed numerical error (lines with symbols) as a function of the one-dimensional cost function $\hat{c}_1$, overlaid with theoretical predictions (dotted lines).

Verification of computational cost estimator

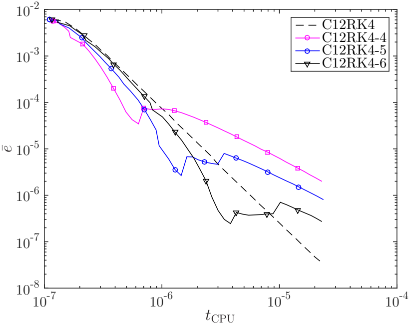

Figure: 9. Numerical error as a function of CPU time for the classical C12RK4 and optimised C12RK4–*n* schemes.

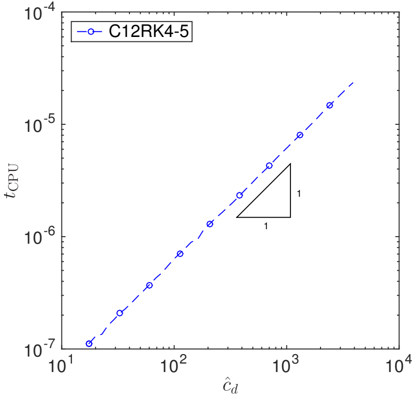

Figure: 10. CPU time compared with cost estimator $\hat{c}_1$.

One-dimensional Gaussian pulse I

Analytical formulation

- Numerical solution of the linear advection equation (26) with $c = 1$.
- Periodic boundary conditions $u(-100, t) = u(100, t)$, $t > 0$.
- Initial condition $u(x, 0) = (1/2)e^{-(x/3)^2}$.
- Broadband spectrum, $\bar{k} = \pi/3$.

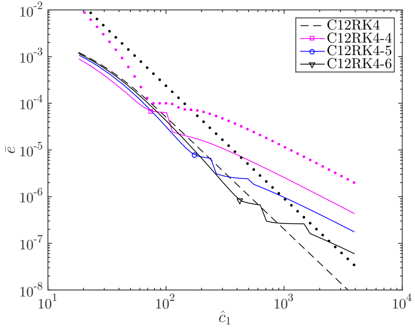

Figure: 11. Numerical error as a function of the one-dimensional cost function $\hat{c}_1$ with error estimates $\hat{e}_a$ overlaid (dotted lines).

One-dimensional Gaussian pulse II

Analytical formulation

- Numerical solution of the linear advection equation (26) with $c = 1$.
- Periodic boundary conditions $u(-100, t) = u(100, t),\ t > 0$.
- Initial condition $u(x, 0) = (1/2)e^{-(x/3)^2}$.
- Broadband spectrum, $\bar{k} = \pi/3$.

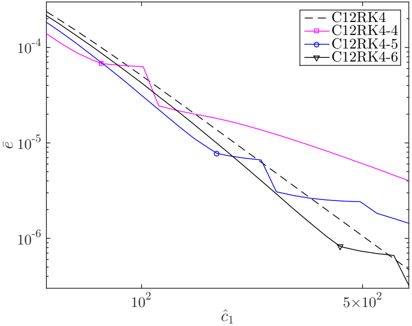

Figure: 12. Detail in the vicinity of the C12RK4-4, C12RK4-5 and C12RK4-6 design points.

1D performance analysis summary

Table: 3. Polychromatic wave. Performance of cost-optimised schemes at their operating points $(\hat{\kappa}^*, \hat{\sigma}^*)$ and comparison with the standard C12RK4 scheme. $\Delta\hat{c}_1(\%)$ and $\Delta\bar{e}(\%)$ indicate the percentage cost and error reduction with respect to the C12RK4 scheme.

Scheme	$\bar{e}$	$\hat{c}_1^*$	$\hat{c}_1^*$ C12RK4	$\Delta\hat{c}_1$ %	$\bar{e}$ C12RK4	$\Delta\bar{e}$ %
C12RK4–4	6.443×10^{-5}	74.376	170.56	56.39	4.706×10^{-4}	86.31
C12RK4–5	7.702×10^{-6}	171.7987	412.19	58.32	6.332×10^{-5}	87.84
C12RK4–6	9.565×10^{-7}	424.136	981.3	56.78	7.191×10^{-6}	86.71

Table: 4. Gaussian pulse. Performance of cost-optimised schemes at their operating points (κ^*, σ^*) and comparison with standard C12RK4 scheme.

Scheme	$\bar{e}$	$\hat{c}_1^*$	$\hat{c}_1^*$ C12RK4	$\Delta\hat{c}_1$ %	$\bar{e}$ C12RK4	$\Delta\bar{e}$ %
C12RK4–4	6.784×10^{-5}	74.677	88.29	15.42	9.954×10^{-5}	31.85
C12RK4–5	7.7647×10^{-6}	173.227	218.78	20.82	1.365×10^{-5}	43.12
C12RK4–6	8.2525×10^{-7}	424.245	554.45	23.48	1.573×10^{-6}	47.54

Two-dimensional Gaussian pulse

Analytical formulation

- Numerical solution of the two-dimensional normalized linearized Euler equations

$$\frac{\partial U}{\partial t} + A_0 \frac{\partial U}{\partial x} + B_0 \frac{\partial U}{\partial y} = 0 \qquad (27)$$

- The unperturbed flow Mach number $M_x = M_y = 0$ [?].
- Eq. (27) is solved in $(-100, 100)^2$.
- Initial conditions are

$$U_0 = \begin{bmatrix} \mathrm{e}^{-\ln(2)(x^2+y^2)/9} \\ 0 \\ 0 \\ \mathrm{e}^{-\ln(2)(x^2+y^2)/9} \end{bmatrix} \qquad (28)$$

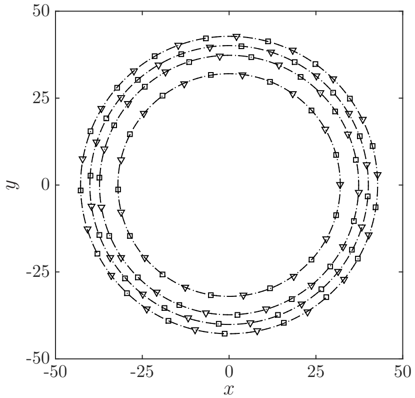

Figure: 13. Propagation of a two-dimensional acoustic pulse in an unbounded domain at non-dimensional $T = 40$, fixed $\sigma = 0.05$.

Verification of computational cost estimator in 2D

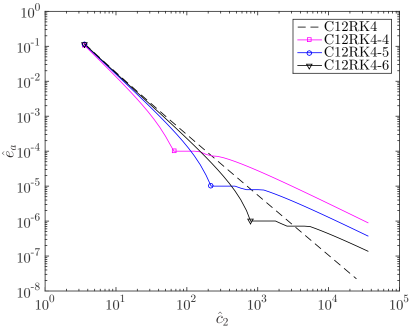

Figure: 14. Comparison of the estimated error $\hat{e}_a$ versus computational cost $\hat{c}_2$.

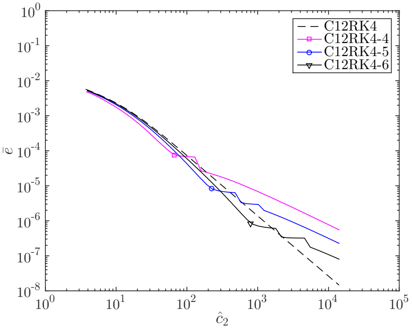

Figure: 15. Computed numerical error (lines with symbols) as a function of two-dimensional cost function $\hat{c}_2$.

2D performance analysis summary

Table: 5. Theoretical performance of cost-optimised schemes for different target errors in two dimensional space. $\Delta\hat{c}_2(\%)$ and $\Delta\hat{e}_a(\%)$ indicate the estimated percentage cost and error reduction with respect to the C12RK4 scheme.

Scheme	$\tilde{\epsilon}$	$\hat{c}_2^*$	$\hat{c}_2^*$ C12RK4	$\Delta\hat{c}_2$ %	$\hat{e}_a$ C12RK4	$\Delta\hat{e}_a$ %
C12RK4–4	10^{-4}	65.69	187.19	64.91	6.215×10^{-4}	83.91
C12RK4–5	10^{-5}	219.98	708.56	68.95	7.557×10^{-5}	86.77
C12RK4–6	10^{-6}	792.86	2699.30	70.63	8.238×10^{-6}	87.86

Table: 6. Two-dimensional Gaussian pulse. Performance of cost-optimised schemes at their design point $(\hat{\kappa}^n_{\mathrm{opt}}, \hat{\sigma}^n_{\mathrm{opt}})$ and comparison with the standard C12RK4 scheme. $\Delta\hat{c}_2(\%)$ and $\Delta\bar{e}(\%)$ indicate the percentage cost and error reductions with respect to the C12RK4 scheme.

Scheme	$\bar{e}$	$\hat{c}_2^*$	$\hat{c}_2^*$ C12RK4	$\Delta\hat{c}_2(\%)$ %	$\bar{e}^*$ C12RK4	$\Delta\bar{e}$ %
C12RK4–4	7.581×10^{-5}	66.93	97.85	31.61	1.449×10^{-4}	47.67
C12RK4–5	8.297×10^{-6}	221.72	352.74	37.14	1.850×10^{-5}	55.16
C12RK4–6	8.540×10^{-7}	799.93	1317.42	39.28	2.020×10^{-6}	57.73

Outline of the presentation

1. Context, Aim and Objectives
   - Context
   - Aim and Objectives
2. Numerical Background
   - Model problem
   - Spatial Discretization
   - Time marching scheme
   - Performance analysis of finite-difference schemes
   - Cost-performance trade-off for CAA algorithms
   - Approximate spatial and temporal error analysis
3. Optimization criteria
   - Optimization of finite-difference schemes
   - Extension to prefactored schemes
   - Optimization of the temporal solver
   - Predicted performance of the combined schemes
4. Applications
   - Polychromatic wave propagation
   - One-dimensional Gaussian pulse
   - 1D performance analysis summary
   - Two-dimensional Gaussian pulse
   - 2D performance analysis summary
5. **Conclusion**
6. Track record on cost-optimized schemes and further/on-going work

Conclusions

Conclusions

- Cost-optimized prefactored compact time-marching schemes C12RK4-n have been developed based on a-priori cost and error estimates.
- Numerical experiments on 1D and 2D problems verified the cost-advantage of the optimized schemes.
- On a polychromatic wave test, $> 50\%$ cost reduction is achieved by C12RK4-n for the same level of error.
- On the broadband test of a Gaussian pulse, between 15% and 20% cost reduction is obtained.
- The cost estimator $\hat{c}_d$ is found to be a good predictor of the actual CPU time saved.

Outline of the presentation

1. Context, Aim and Objectives
    - Context
    - Aim and Objectives
2. Numerical Background
    - Model problem
    - Spatial Discretization
    - Time marching scheme
    - Performance analysis of finite-difference schemes
    - Cost-performance trade-off for CAA algorithms
    - Approximate spatial and temporal error analysis
3. Optimization criteria
    - Optimization of finite-difference schemes
    - Extension to prefactored schemes
    - Optimization of the temporal solver
    - Predicted performance of the combined schemes
4. Applications
    - Polychromatic wave propagation
    - One-dimensional Gaussian pulse
    - 1D performance analysis summary
    - Two-dimensional Gaussian pulse
    - 2D performance analysis summary
5. Conclusion
6. Track record on cost-optimized schemes and further/on-going work

Track record and further/on-going work I

Track record on cost-optimized schemes

- [?] S. Pirozzoli: *Performance analysis and optimization of finite difference schemes for wave propagation problems*, Journal of Computational Physics, 222:809-831, 2007.
- [?] Rona & al.: *Comparison of optimized high-order finite-difference compact schemes for computational aeroacoustics* conference paper 2009-0498, 47^{th} Aerospace Sciences Meeting and Exhibit, Orlando, Florida.
- [?] M. Bernardini & S. Pirozzoli: *Space- and time-optimized schemes for computational aeroacoustics* conference paper 2009-3481, 13^{th} Aeroacoustics Conference, Rome, Italy.
- [?] M. Bernardini & S. Pirozzoli: *A general strategy for the optimization of Runge-Kutta schemes for wave propagation phenomena*, Journal of Computational Physics, 228:4182-4199, 2009.
- [?] I. Spisso: *Development of a prefactored high-order compact scheme for low-speed aeroacoustics* PhD Thesis, University of Leicester, December 2013
- [?]: *Development of a prefactored high-order compact scheme for low-speed aeroacoustics*, SIMAI 2014, Taormina, Italy.
- [?]: *Optimized prefactored compact schemes for wave propagation phenomena*, conference paper 2016-2721, 22^{th} Aeroacoustics Conference, Lyon, France.
- [?]: *Optimized prefactored compact schemes for wave propagation schemes*, SIMAI 2016, Milan, Italy.
- A. Rona, I. Spisso, E. Hall, S. Pirozzoli, M. Bernardini: *Optimized prefactored compact schemes for wave propagation phenomena*, Under consideration for publication *Journal of Computational Physics*

Track record and further/on-going work II

To do List

- Extension to real flow physics:
  - Boundary conditions effects
  - three-dimensionality
  - non-linearity
- Implement a slab decomposition (no error introduced by the parallelization strategy to be used into HPC cluster, 2D pencil domain decomposition). [**?**, **?**]).

Bernardini, M. & Pirozzoli, S. (2009). A general strategy for the optimization of Runge-Kutta schemes for wave propagation phenomena. *Journal of Computational Physics*, **228**, 4182–4199.

Bogey, C. & Bailly, C. (2004). A family of low dispersive and low dissipative explicit schemes for flow and noise computations. *Journal of Computational Physics*, **194**, 194–214.

Butcher, J.C. (1987). *The Numerical Analysis of Ordinary Differential Equations: Runge-Kutta and General Linear Methods*. John Wiley & Sons Inc.

Colonius, T. & Lele, S. (2004). Computational aeroacoustics: progress on nonlinear problems of sound generation. *Progress in Aerospace Sciences*, **40**, 365–416.

Guarrasi, M., Frigio, S., Emerson, A. & Erbacci, G. (2013). Scalability Improvements for DFT Codes due to the Implementation of the 2D Domain Decomposition Algorithm. Tech. rep., PRACE White Paper available at `http://www.prace-ri.eu/IMG/pdf/wp85.pdf`.

Hirsch, C. (2007). *Numerical Computation of Internal and External flow*, vol. 1, Fundamental of Computational Fluid Dynamics. New York, 2nd edn.

Hixon, R. (2000). Prefactored small-stencil compact schemes. *Journal of Computational Physics*, **165**, 522–41.

HU, F.Q., HUSSAINI, M.Y. & MANTHEY, J.L. (1996). Low-dissipation and low-dispersion Runge-Kutta schemes for computational acoustics. *Journal of Computational Physics*, **124**, 177–191.

LELE, S.K. (1992). Compact finite difference schemes with spectral-like resolution. *Journal of Computational Physics*, **103**, 16–42.

LI, N. & LAIZET, S. (2010). 2DECOMP&FFT – A highly scalable 2D decomposition library and FFT interface. Tech. Rep. Cray User Group 2010 conference.

PIROZZOLI, S. (2007). Performance analysis and optimization of finite-difference schemes for wave propagation problems. *Journal of Computational Physics*, **222**, 809–831.

PIROZZOLI, S. & BERNARDINI, M. (2007). Space- and time-optimized schemes for computational aeroacoustics. Conference paper, AIAA/CEAS Aeroacoustics Conference13th, Rome, Italy.

RONA, A. & SPISSO, I. (2007). Implementation of a high-order finite difference scheme to model wave propagation. Conference paper 2007-3487, AIAA/CEAS Aeroacoustics Conference13th, Rome.

RONA, A., SPISSO, I., BERNARDINI, M. & PIROZZOLI, S. (2009). Comparison of optimized high-order finite-difference compact scheme for computational aeroacoustics. Conference paper 2009-0498, Aerospace Sciences Meeting and Exhibit47th, Orlando, Florida.

Rona, A., Hall, E.J.C. & Spisso, I. (2016). Optimized prefactored compact schemes for wave propagation phenomena. Tech. Rep. 2016-2721, 22^{th} AIAA/CEAS Aeroacoustics Conference, Lyon, France.

Spisso, I. (2013). *Development of a Prefactored High-Order Compact Scheme for Low-Speed Aeroacoustics*. Ph.D. thesis, University of Leicester, Le1 7HR, optional.

Spisso, I., Rona, A. & Pirozzoli, S. (2014). Development of a prefactored high-order compact scheme for low-speed aeroacoustics. SIMAI 2014, Biannual Congress of the Società Italiana di Matematica Applicata e Industriale.

Spisso, I. *et al.* (2016). Optimized prefactored compact schemes for wave propagation phenomena. No. C15 in SIMAI 2016, Biannual Congress of the Società Italiana di Matematica Applicata e Industriale.